Qualification of turbine architectures in a multiphysical approach: application to a turboshaft engine

Laurent Pierre, Denis Teissandier, Jean-Pierre Nadeau

Qualification of turbine architectures in a multiphysical approach: application to a turboshaft engine

Laurent Pierre [1], Denis Teissandier [2], Jean Pierre Nadeau [3]

(1), (3) : Arts et Métiers ParisTech
Esplanade des Arts et Métiers
33405 Talence Cedex – France
Phone/Fax: 33-5-56845428/5436
E-mail: {Laurent.Pierre, jean-pierre.nadeau}@bordeaux.ensam.fr

(2) : Université de Bordeaux
351, cours de la Libération
33405 Talence Cedex - France
Phone/Fax: 33-5-40006220/6964
E-mail: denis.teissandier@u-bordeaux1.fr

Abstract: The performance of a turboshaft engine derives essentially from the performance of the turbine, which in turn is closely correlated with rotor/stator clearance at the blade tips. In this article we propose to define criteria for qualifying turbine architectures based on a geometric model which integrates variability due to the processes of obtaining parts, the assembly processes and the thermomechanical behaviour of the turbine. The geometric model proposed here integrates thermomechanical strains in 3D dimension-chains formalised by operations on polytopes (Minkowski sum and intersection).

Key words: geometric variability, tolerancing analysis, thermomechanics, performance criteria

1- Introduction

Controlling the behaviour and the energy yield of turboshaft engines for each of the different operating regimes is essential to ensure that the desired power is achieved. One way to improve the performance of these turboshaft -engines is to control the geometric variability of the turbine, and more particularly the clearance between the blade tips and the stator.

In the preliminary design phase, several alternative turbine architectures are envisaged. These alternatives are often based on different component shapes and dimensions, with several technical solutions being proposed for joints between components and different materials. In this article we propose a model which will define clearance between blade tips and stator for different turbine architectures, taking the following variabilities into account:

-processes for obtaining parts,
-processes for assembling parts,
- thermomechanical behaviour of the turbine.

Two performance criteria are formulated with which to qualify the proposed solutions: risk of touching and leakage section between rotor and stator. This work is part of a general series of studies into decision support systems to assist the designer in choosing a qualified turbine architecture that performs better than any other.

In the first part, the procedure for modelling different geometric variabilities is described. In the second part the qualification criteria for turbine architectural solutions are presented. In the third part, we describe an application of this work to a sub-unit of a turbine of turboshaft engine.

Finally, after drawing the principal conclusions, future developments for this work are presented.

2- Modelling geometric variability

The geometric variability in processes for obtaining parts and in assembly processes are taken into account by 3D dimension chain simulation tools. However, most of these tools model the different parts as infinitely rigid solids, so to make up for this, the thermomechanical strains on the parts must be integrated into 3D dimension chain simulations. This is essential in order to control clearance at the tip of the turbine blade in different operating phases in a turboshaft engine [PT1].

2.1 – Variability due to manufacturing and assembly processes

The geometric models used in 3D dimension chains are generally based on the following hypotheses: no defect in the shape of the real surfaces, no local strain on surfaces in contact and no flexible parts. The limits for geometric defects in a part (defined by specification), and acceptable limits for relative displacement between two surfaces in contact (defined by clearance) are formalised mathematically by a small displacement torsor [BB1] and [CB1], a matrix [T1], deviation hulls [GD1] and clearance [GS1] or T-Maps [MD1], [JA1]. In the following part of the article, hulls will

be modelled using polytopes [TD1].

2.2 – Variability due to thermomechanical behaviour

Several studies have been carried out to manage compliant structure: [JC1], [SC1], [SL1] and [XW1]. These works take into account geometric variations induced by the assembly process and manufacturing dispersions. [MS1] and [MS2] show the interest of considering functional requirement variations along the various phases of the product life cycle. Simulation of the thermomechanical behaviour of the system studied is based on finite element digital simulations.

Let us consider the 3D dimension chain system which characterises a functional requirement, where the parts are all considered as infinitely rigid (reference behaviour). This system includes intersections and Minkowski sums for polytopes which define acceptable limits of deviation in the parts and acceptable limits of displacement between two parts potentially in contact [PT2]. This system is referred to as the reference system in the reference behaviour [PT1].

Our hypothesis is that the topological structure of the contacts graph in the reference behaviour and all thermomechanical behaviours remain the same. This means that there is no extra contact and no suppression of contact between the two behaviours. On the other hand, the different parameters that determine contact (minimal clearance, maximal clearance and nature of contact) may change.

Each thermomechanical behaviour is characterised by a specific 3D dimension chain system. A 3D dimension chain system for a given behaviour is deduced from the reference system:

- by updating the clearance hulls, taking into account changes in the different contact parameters from rigid behaviour (see Figure 1) to thermomechanical behaviour (Figure 2).
- by updating deviation hulls to incorporate displacements caused by thermomechanical strains and the acceptable limits for geometrical defects by superimposition [PT2] (see Figure 3).

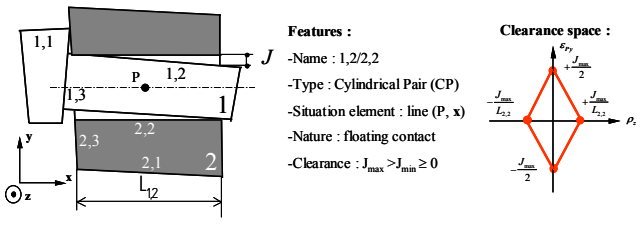

Figure 1: Cylindrical pair contact in rigid behaviour

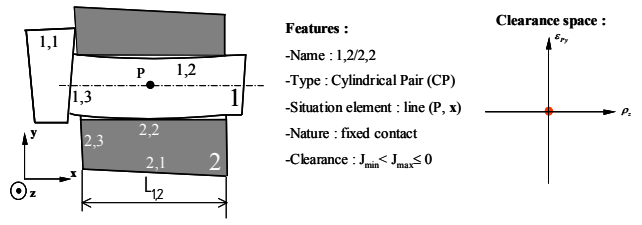

Figure 2: Cylindrical pair contact in thermomechanical behaviour

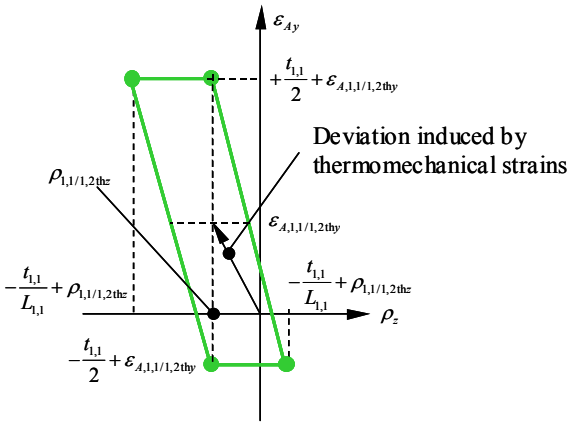

Figure 3: Deviation hull incorporating thermomechanical strains

Thermomechanical stresses on the parts lead to strains in the free surfaces, i.e. the surfaces not in contact with other surfaces. Deviations of thermomechanical origin in the shape of the free surfaces are taken into account in the 3D dimension chain modelling. A deviation in shape will be characterised by the local distance between a point on the real surface and the associated substitute surface.

3- Turbine performance criteria

3.1 –Correlation of performance criteria with geometrical criteria

The correct functioning of a turbine relies on two performance criteria: energy yield and the risk of a blade touching the stator. These two performance criteria depend on the clearance between the turbine blades and the stator. Turbine energy yield is correlated with the flow of gas between the blade tips and the stator. This flow rate depends on the leakage section, the difference between the rotor and the stator sections; in order to guarantee optimal yield, it must not exceed a maximal value: $S_{\max}$.

To maximise the turbine's energy yield, rotor-stator clearance should be as small as possible while ensuring that in all of the turbine's operational phases the blades are not too close to the stator (which could damage the turbine and risk damaging the engine in operation). The risk of touching is correlated with a minimal clearance value that must be respected: $C_{\min}$.

3.2 –Geometrical criteria

Local clearance between the blades and the stator $C(\theta)$ should be sufficient to avoid touching any part of the periphery of the turbine (see Figure 4).

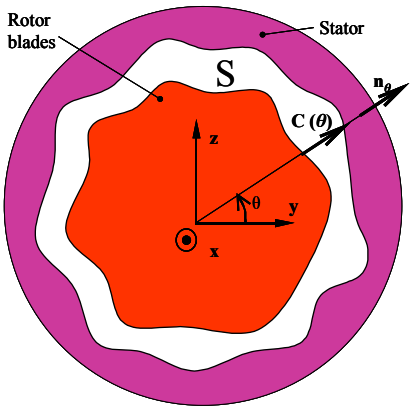

Figure 4 : Sections of the rotor blades and the stator.

The touch criterion can be expressed by the following equation, where C_{min} is the minimum clearance that guarantees that the turbine functions correctly.

$$C(\theta) > C_{min} \quad \theta \in [0;2\pi[\tag{1}$$

The leaking of gas between the stator and the rotor is determined by the leakage section S (see Figure 4).

The criterion for power in a turbine is correlated with the leakage section. To maximise turbine power the leakage section must be minimised, as defined in the following equation:

$$S < S_{\max} \quad \text{avec } S = S_{stator} - S_{rotor} \tag{2}$$

S_{stator} defines the section of the ring that is close up to the rotor, with the section of the rotor expressed as S_{rotor} .

3.3 – Stator variability

$\boldsymbol{\delta}(M,\theta)$ defines the position of a point on the real profile, with M the centre of the least squares circle and according to angle θ , in relation to the reference axis (Figure 5).

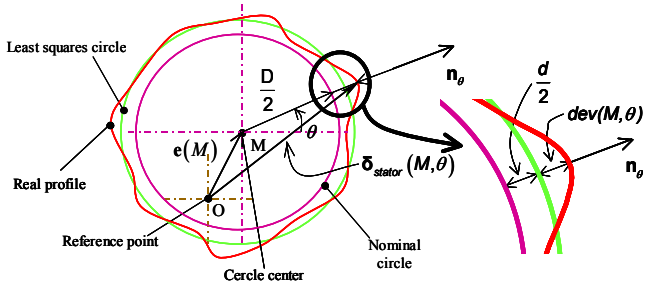

Figure 5: Parameters of a nominal circular surface

The position $\boldsymbol{\delta}(M,\theta)$ is written:

$$\boldsymbol{\delta}_{stator}(M,\theta) = \mathbf{e}(M) + \left(\frac{\mathrm{D}}{2} + \frac{d}{2} + dev(M,\theta)\right).\mathbf{n}_\theta \tag{3}$$

The preceding equation is defined as follows:

- $\mathbf{e}(M)$: location deviation of the centre of the substitute circle in relation to the reference point
- D : nominal diameter
- d : dimension deviation between the nominal diameter and the substitute circle diameter
- $dev(M,\theta)$: shape deviation of the real profile in relation to the substitute circle.

By integrating equation (3) into equation (1), the touch criterion can be defined by the following equation:

$$\mathbf{C}(\theta) = \begin{cases} \mathbf{e}(M) + \left(\frac{\mathrm{D}}{2} + \frac{d}{2} + dev(M,\theta)\right).\mathbf{n}_\theta \\ -\boldsymbol{\delta}_{rotor}(M,\theta) \end{cases} \tag{4}$$

avec : $\theta \in [0;2\pi[$

By combining equation (3) with equation (2), which describes the stator, the energy yield criterion is then defined as:

$$S = \int_0^{2\pi} \frac{1}{2}.\left(\frac{\mathrm{D}}{2} + \frac{d}{2} + dev(M,\theta)\right)^2 .d\theta - S_{rotor} \tag{5}$$

The deviations in dimension and shape are very small compared with the nominal diameter of the stator section. The integral which formalises the area of the stator section in equation (5) can then be linearised:

$$S_{stator} = \pi \times \left(\frac{\mathrm{D}}{2}\right)^2 + \frac{\mathrm{D}}{2} \times \int_0^{2\pi} \left(\frac{d}{2} + dev(M,\theta)\right).d\theta \tag{6}$$

4- Application to a simplified turbine model

4.1 - Description of the simplified turbine

The simplified model of the turbine (Figure 6) consists of two sub-units: a stator (parts labelled 1 and 2) and a rotor (part labelled 3), with a turning pair contact around **x**: see Figure 6. Part 3 forms a revolution, where the largest diameter corresponds to the diameter of the blade tips.

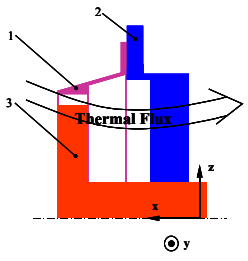

Figure 6: Simplified geometric model of a turbine.

When the engine is in operation, a flow of hot gases (1000°C approx.) is created by the combustion chamber (not shown in Figure 6) and as a result parts 1, 2 and 3 undergo strain. In this example, only the thermomechanical strains on part 1 are

taken into account when the engine is in operation.

In the following part of the article, parts 2 and 3 are by assumption considered as infinitely rigid and geometrically perfect. Moreover, the turning pair contact between part 2 and part 3 is considered to have no defects and no clearance.

The criteria defined in §2 will be studied for two different turbine architectures. Two variants of a technical solution will be considered, the aim being to produce a clamping contact between part 1 and part 2 (see Figure 7):

- Architecture 1: planar pair contact with five short centring plugs located on a diameter D and distributed equiangularly.
- Architecture 2: planar pair contact with one short centring plug.

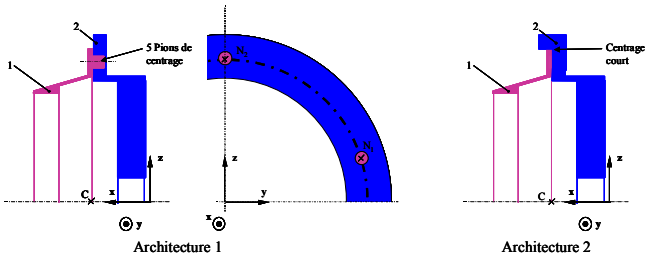

Figure 7: Turbine architectures.

4.2 – Defining parameters and formulating performance criteria

According to the hypotheses defined in the previous paragraph, the geometric variabilities of the two technical solutions considered depend only on the processes of obtaining part 1, and assembling parts 1 and 2 together, and the thermomechanical behaviour of part 1.

Equation (5) defines the touch criterion; this then becomes:

$$C(\theta) = \Delta C(\theta) + C_0 \text{ avec :}$$
$$\Delta C(\theta) = \mathbf{e}(M).\mathbf{n}_\theta + \frac{d}{2} + dev(M,\theta) \quad (7)$$
$$C_0 = \frac{\mathrm{D}}{2} - \boldsymbol{\delta}_{stator}(M,\theta).\mathbf{n}_\theta$$

Equation (6) defining the energy yield criterion then becomes:

$$S = \Delta S + S_0$$
$$\text{avec : } \Delta S = \frac{\mathrm{D}}{2} \times \int_0^{2\pi} \left(\frac{d}{2} + dev(M,\theta) \right) . d\theta \quad (8)$$
$$\text{et : } S_0 = \pi \times \left(\frac{\mathrm{D}}{2} \right)^2 - S_{rotor}$$

$\Delta C(\theta)$ and ΔS are dependent on the architecture variants. C_0 and S_0 are variables that are independent of the architectures.

4.3 – Geometric characterisation

In the first phase, the turbine is modelled in a reference behaviour where all the solids are infinitely rigid: only manufacturing defects and clearance in the different contacts is taken into account. In phase two, a thermomechanical behaviour is considered, where there are strains due to the flow of hot gases from the combustion chamber at a point when the turbine is operating in a steady regime. Thermomechanical strains are then integrated into the reference model as described in §2.2.

4.3.1 Characterisation of the variability of production and assembly processes

Figure 8 describes the two architectures considered.

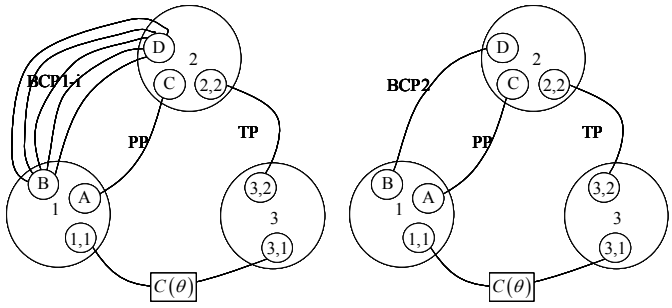

Features of BCP1-i ($1 \le i \le 5$)
-Name : 1,i/2,i
-Type : Ball and Cylinder Pair (BCP)
-Situation element : point N_i, line (N_i, x)
-Nature : floatting contact
-Clearance : $0 \le J_{min} \le J_{max}$

Features of BCP2
-Name : 1,1/2,1
-Type : Ball and Cylinder Pair (BCP)
-Situation element : point C, line (C, x)
-Nature : floatting contact
-Clearance : $0 \le J_{min} \le J_{max}$

Features of PP
-Name : 1,7/2,7
-Type : Planar Pair (PP)
-Situation element : line (C, x)
-Nature : sliding contact
-Clearance : $J_{max} = J_{min} = 0$

Features of TP
-Name : 1,7/2,7
-Type : Turning Pair (PP)
-Situation element : line (C, x)
-Nature : sliding contact
-Clearance : $J_{max} = J_{min} = 0$

Figure 8: Graphs of contacts.

For architecture 1, the clamping contact consists of a planar pair contact and five ball and cylinder pair contacts, with clearance, by means of five centring slugs. For architecture 2, the clamping contact consists of a planar pair contact and one ball and cylinder pair contact, with a clamping screw.

In both architectures, bolts are used to keep parts 1 and 2 in position. They are not considered in the modelling process as they do not affect the relative positioning of parts 1 and 2.

Determination of: $e(M) = \mathbf{e}(M).\mathbf{n}_\theta$ is based on a 3D dimension chain formalised by operations on the hulls (intersections and Minkowski sums).

The hull that defines the displacement limits of surface 1,1 in relation to surface 3,1 is expressed by the following Minkowski sum:

$$\mathfrak{D}_{1,1/3,1} = \mathfrak{D}_{1,1/AB} + \mathfrak{D}_{AB/CD} + \mathfrak{D}_{CD/2,2} + \mathfrak{D}_{2,2/3,2} + \mathfrak{D}_{3,2/3,1} \quad (9)$$

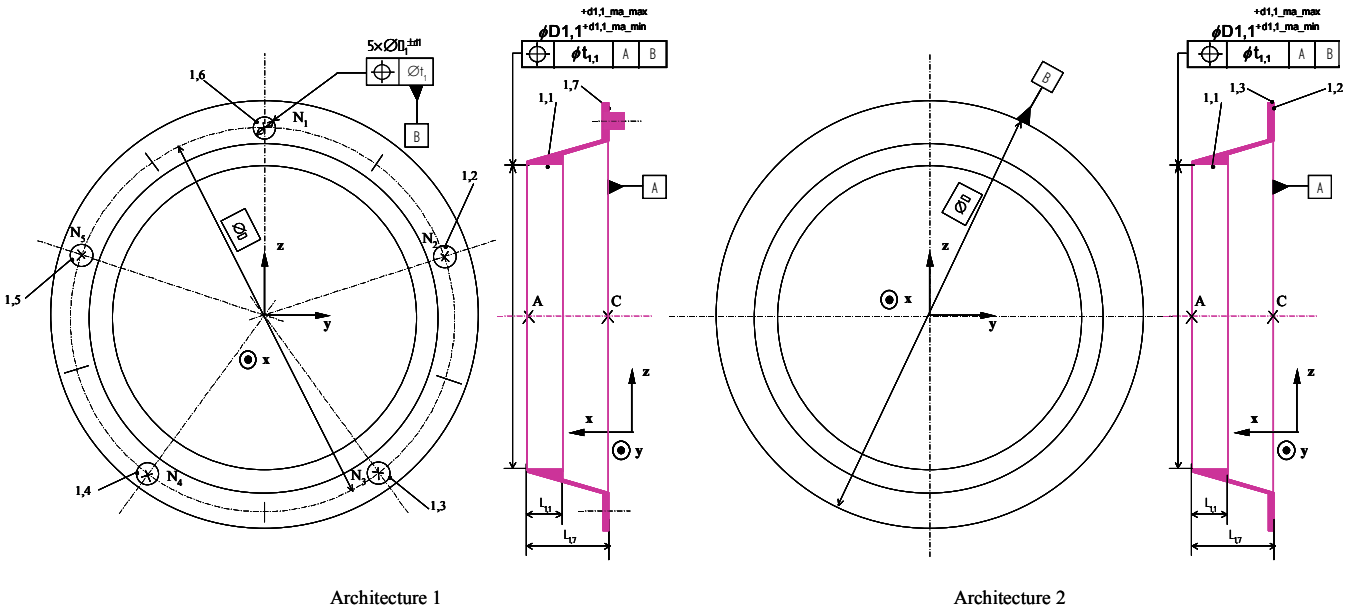

Figure 9: Definitions of parts 1.

$\mathfrak{D}_{AB/CD}$ is the clearance hull defined by the planar pair contact and the five ball and cylinder pair contacts for architecture 1 and the one ball and cylinder pair contact for architecture 2. $\mathfrak{D}_{1,1/AB}$ is the deviation hull characterised by the location of surface 1,1 in relation to reference system AB according to ISO standards [I3], [I1] and [I2]. for the two architectures (see Figure 9). Hulls $\mathfrak{D}_{CD/2,2}$ and $\mathfrak{D}_{3,2/3,1}$ characterise the deviation hulls for parts 2 and 3 respectively, and hull $\mathfrak{D}_{2,2/3,2}$ characterises the clearance hull for the turning pair contact between parts 2 and 3.

According to the hypotheses advanced in §4.1, equation (9) then becomes:

$$\mathfrak{D}_{1,1/3,1} = \mathfrak{D}_{1,1/AB} + \mathfrak{D}_{AB/CD} \tag{10}$$

Deviation hulls $\mathfrak{D}_{1,1/3,1}$, resultants from the Minkowski sums defined by equation (10), are shown in Figure 10, where J_{max} represents clearance in the five ball and cylinder pair contacts and $t_{1,1}$ the dimension of the tolerance zone for the location specification of surface 1,1.

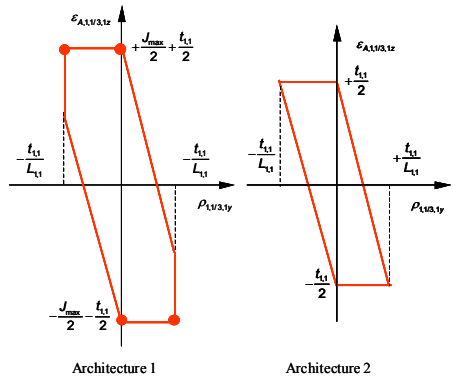

Figure 10: Deviation hull of location of surface 1,1 at point A.

From Figure 10 we are able to determine the values of the location deviation between surfaces 1,1 and 2,1. Equations (11) and (12) define the minimal values of this deviation for architecture 1 and architecture 2 respectively:

$$-\frac{J_{\max}}{2}-\frac{t_{1,1}}{2} \le e_{\text{stator\_A1}}(M) \le +\frac{J_{\max}}{2}+\frac{t_{1,1}}{2} \tag{11}$$

$$-\frac{t_{1,1}}{2} \le e_{\text{stator\_A2}}(M) \le +\frac{t_{1,1}}{2} \tag{12}$$

As seen in the definition drawing for part 1, the dimension deviations for surface 1,1 in both architectures are given in equations (13) and (14).

$$\mathrm{d}_{1,1\_\mathrm{ma\_min}} \le d_{\text{stator\_A1}} \le \mathrm{d}_{1,1\_\mathrm{ma\_max}} \tag{13}$$

$$\mathrm{d}_{1,1\_\mathrm{ma\_min}} \le d_{\text{stator\_A2}} \le \mathrm{d}_{1,1\_\mathrm{ma\_max}} \tag{14}$$

By definition, deviations in shape due to manufacture are not taken into account, which gives:

$$dev_{\text{stator\_A1}}(M,\theta) = dev_{\text{stator\_A2}}(M,\theta) = 0 \tag{15}$$

4.3.2 Characterisation of thermomechanical variability

Thermomechanical strains caused by a flow of gases from the combustion chamber and illustrated in Figure 11 have to be integrated into the geometric variability of the stator.

A preliminary thermal study can determine any change in the joint between part 1 and part 2. As described by [PT1] and [PT2], the nature of the contacts and the clearances may change from one behaviour to another.

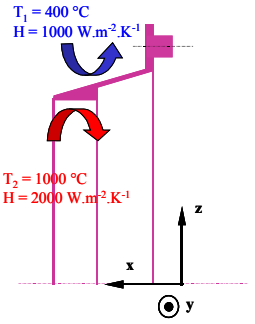

Figure 11: Thermal marginal conditions

In the case of architecture 1, the radial displacement of the slugs in their housing uses up all the clearance (see Figure 12).

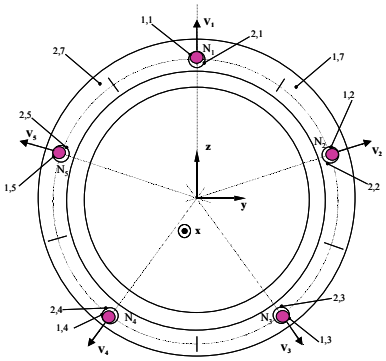

Figure 12 : Radial displacements of the slugs

The planar pair contact / short centring, used in the technical solution for architecture 2, remains without clearance.

A thermomechanical analysis of part 1 was carried out with the thermal limit conditions defined in Figure 11 and the mechanical limit conditions defined in Figure 8.

After a thermomechanical calculation of finite elements using the Samcef software, the geometry of the deformation of surface 1,8 was studied in section for each of the architectures (see Figure 13).

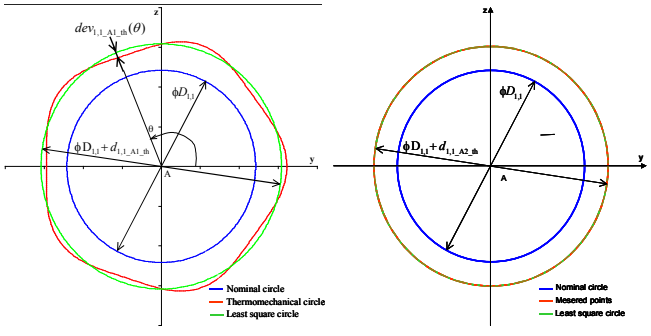

Architecture 1 Architecture 2

Figure 13: Thermomechanical strains of surface 1,1 in plane $(A, \mathbf{x})$

From Figure 13 we can determine location deviation, dimension deviation and shape deviation, due to thermomechanical strain for both architectures.

When changes in contacts, changes in geometry, and the different deviations defined in equations (11) to (15) are incorporated, this gives:

$$-\frac{t_{1,1}}{2} \le e_{stator\_A1}(M) \le +\frac{t_{1,1}}{2} \quad (16)$$

$$-\frac{t_{1,1}}{2} \le e_{stator\_A2}(M) \le +\frac{t_{1,1}}{2} \quad (17)$$

$$d_{1,1\_ma\_min} + d_{1,1\_A1\_th} \le d_{stator\_A1} \le d_{1,1\_ma\_max} + d_{1,1\_A1\_th} \quad (18)$$

$$d_{1,1\_ma\_min} + d_{1,1\_A2\_th} \le d_{stator\_A2} \le d_{1,1\_ma\_max} + d_{1,1\_A2\_th} \quad (19)$$

$$dev_{1,1\_A1\_th\_min} \le dev_{stator\_A1}(M,\theta) \le dev_{1,1\_A1\_th\_max} \quad (20)$$

$$dev_{stator\_A2}(M,\theta) = 0 \quad (21)$$

4.3.3 Application to two alternative architectures

All the parameters defining the variability of clearance at the blade tips as a function of geometric and architectural variability have been defined. These different parameters are then exploited to compare the two architectures one with another in terms of thermomechanical situation.

From equations (22) and (23), for thermomechanical behaviour, we can compare variations in minimal clearance for the two architectures.

$$\left.\begin{aligned} &-\frac{t_{1,1}}{2} + d_{1,1\_ma\_min} + d_{1,1\_A1\_th} \\ &+dev_{1,1\_A1\_th\_min} + C_0 \end{aligned}\right\} > C_{min} \quad (22)$$

$$-\frac{t_{1,1}}{2} + d_{1,1\_ma\_min} + d_{1,1\_A2\_th} + C_0 > C_{min} \quad (23)$$

From equations (24) and (25) we can compare the energy yield of the two architectures, from variations in the leakage sections.

$$\pi \times D_{stator} \times \frac{d_{1,1\_ma\_min} + d_{1,1\_A1\_th}}{2} + S_0 < S_{max} \quad (24)$$

$$\pi \times D_{stator} \times \frac{d_{1,1\_ma\_min} + d_{1,1\_A2\_th}}{2} + S_0 < S_{max} \quad (25)$$

To compare the two architectures in terms of thermomechanical behaviour, only dimension deviations and shape deviations are determinant in relation to the two performance criteria. Thermomechanical calculations give the following results:

$$d_{1,1\_A1\_th} < d_{1,1\_A2\_th} \text{ et } dev_{1,1\_A1\_th\_min} < 0 \quad (26)$$

Where the risk of touching predominates over energy yield, architecture 2 is the most efficient.

Where energy yield predominates over the risk of touching, then architecture 1 performs best.

Thus the preponderance of one or other of the two performance criteria determines which is the more efficient solution.

5- Conclusions-Perspectives

In this article we have defined the geometrical variability of a turbine using a multiphysical approach, and including the variability of processes associated with obtaining parts, assembly processes and the thermomechanical behaviour of the turbine. Variants of technical solutions for joints between the ring and the turbine housing have been formalised. Two performance criteria were used, risk of touching the stator and energy yield, to qualify the solutions envisaged.

One of the future perspectives for this work will be to combine variants of technical solutions for joints with geometrical variants (shape and nominal dimensions of parts). The multiphysical geometrical analysis used in this article can be applied to all types of mechanical systems.

6- References

[BB1] Bourdet P. and Ballot E. Geometrical behavior laws for computer aided tolerancing. In 4th CIRP Seminar on Computer Aided Tolerancing (ed. F. Kimura): 143-153, 1995

[CB1] Clément A. and Bourdet, P. A Study of optimal-criteria identification based on the small-displacement screw model. In Annals of the CIRP,Vol. 37/1/1988, 1988.

[GD1] Giordano M. and Duret D. Clearance Space and Deviation Space, Application to three-dimensional chains of dimensions and positions, In 3rd CIRP Seminar on Computer Aided Tolerancing, ISBN 2-212-08779-9: 179-196, Eyrolles, 1993.

[GS1] Giordano M., Samper S. and Petit J.P. Tolerance analysis and synthesis by means of deviation domains, axi-symetric cases. In 9th CIRP Seminar on Computer Aided Tolerancing, ISBN 978-1-4020-5437-2: 85-94, Springer, 2005.

[I1] ISO 1101, Geometrical Product Specifications (GPS), Geometrical tolerancing, Tolerances of form, orientation, location and run-out, 2004.

[I2] ISO 5459, Technical drawings, Geometrical tolerancing, Datums and datum-systems for geometrical tolerances, 1981.

[I3] ISO 8015, Technical drawings, Fundamental tolerancing principle, 1985.

[JA1] Jian A. D., Ameta G., Davidson J. K. and Shah J. J. Tolerance Analysis and Allocation using Tolerance-Maps for a Power Saw Assembly, In 9th CIRP Seminar on Computer Aided Tolerancing, ISBN 978-1-4020-5437-2: 267-276, Springer, 2005.

[JC1] Jack Hu S. and Camelio J. Modeling and Control of Compliant Assembly Systems. In CIRP Annals, Manufacturing Technology, 55 (1): 19-22, 2006.

[MD1] Mujezinovi A., Davidson J-K. and Shah J-J. A new mathematical model for geometric tolerances as applied to round faces, In ASME Transactions on Journal of Mechanical Design, 126: 504–518. 2004.

[MS1] Mandil G., Desrochers A. and Rivière A. Computational methodology for the prediction of functional requirement variations across the product life-cycle. 11th CIRP Seminar on Computer Aided Tolerancing, Proceedings of the conference, Annecy - France, 2009.

[MS2] Mandil G., Serré P., Desrochers A., Clément A. and Rivière A. Parametric Approach for Geometrical Requirement Calculation Along the Product Life-Cycle. 20th CIRP Design Conference, Proceedings of the conference, Nantes - France, 2010.

[PT1] Pierre L., Teissandier D. and Nadeau J.-P. Integration of thermomechanical strains into tolerancing analysis, In International Journal on Interactive Design and Manufacturing, (3): 247-263, 2009.

[PT2] Pierre L., Teissandier D. and Nadeau J.-P. Integration of multiple physical behaviours into a geometric tolerancing approach. 11th CIRP Seminar on Computer Aided Tolerancing, Proceedings of the conference, Annecy - France, 2009.

[SC1] Stewart M. L. and Chase K. W. Variation simulation of fixtured assembly for compliant structures using piecewise-linear analysis. In American Society of Mechanical Engineers, Manufacturing Engineering Division, MED Volume 16-1: 591-600, 2005.

[SL1] Söderberg R., Lindkvist L. and Dahlström, S. Computer-aided robustness analysis for compliant assemblies. In Journal of Engineering Design, 17: 411-428, 2006.

[T1] Turner J. U. Relative positioning of parts in assemblies using mathematical programming. In Computer Aided Design, 22: 394-400, 1990.

[TD1] Teissandier D., Delos V. and Couétard Y., Operations on polytopes: application to tolerance analysis, In 6th CIRP Seminar on Computer Aided Tolerancing, ISBN 0-7923-5654-3: 425-433, Kluwer academic publisher, 1999.

[XW1] Xie K., Wells L., Camelio J. A. and Youn B. D. Variation propagation analysis on compliant assemblies considering contact interaction. In Journal of Manufacturing Science and Engineering, Transactions of the ASME, 129 (5): 934-942, 2007.

